



3 4456 0050746 8

Rate-Controlling Factors in the Carbothermic Preparation of UO₂-UC₂-C Microspheres

D. P. Stinton
S. M. Tiegs
W. J. Lackey
T. B. Lindemer

OAK RIDGE NATIONAL LABORATORY

CENTRAL RESEARCH LIBRARY

CIRCULATION SECTION

4500N ROOM 175

LIBRARY LOAN COPY

DO NOT TRANSFER TO ANOTHER PERSON

If you wish someone else to see this
report, send in name with report and
the library will arrange a loan.

UCN-7969 3 9-77

OAK RIDGE NATIONAL LABORATORY
OPERATED BY UNION CARBIDE CORPORATION · FOR THE DEPARTMENT OF ENERGY

ORNL/TM-6589
Distribution
Category UC-77

Contract No. W-7405-eng-26

METALS AND CERAMICS DIVISION

HTGR FUEL RECYCLE DEVELOPMENT PROGRAM (189a OH045)
Fuel Refabrication - Task 500

RATE-CONTROLLING FACTORS IN THE CARBOTHERMIC PREPARATION
OF UO_2 - UC_2 -C MICROSPHERES

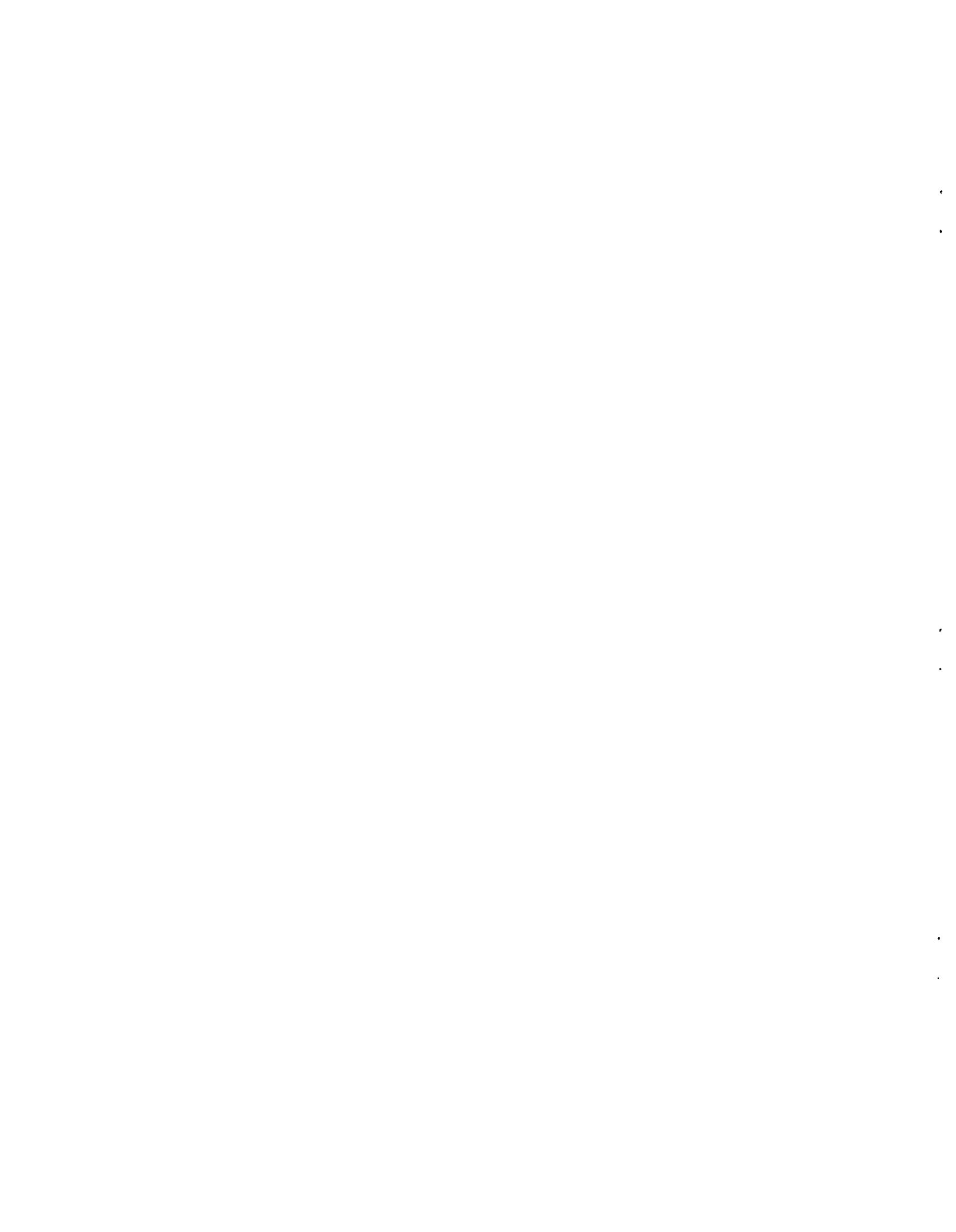
D. P. Stinton, S. M. Tiegs, W. J. Lackey,
and T. B. Lindemer

Date Published: January 1979

Prepared by the
OAK RIDGE NATIONAL LABORATORY
Oak Ridge, Tennessee 37830
operated by
UNION CARBIDE CORPORATION
for the
DEPARTMENT OF ENERGY



3 4456 0050746 8



CONTENTS

	<u>Page</u>
ABSTRACT	1
INTRODUCTION	1
PROCEDURE	3
RESULTS AND DISCUSSION	4
Mass Spectrometry	4
X-Ray Diffraction	9
Metallography	10
Ion Microprobe	11
CONCLUSIONS	11
ACKNOWLEDGMENTS	12
REFERENCES	12
APPENDIX	15

RATE CONTROLLING FACTORS IN THE CARBOTHERMIC PREPARATION
OF UO₂-UC₂-C MICROSPHERES

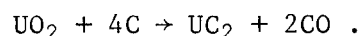
D. P. Stinton, S. M. Tiegs, W. J. Lackey,
and T. B. Lindemer*

ABSTRACT

Rate controlling factors in the conversion of UO₂ + C microspheres to UC₂ + C were investigated using a 13-cm-diam fluidized bed furnace. X-ray diffraction, ion microprobe, and microstructural examination revealed that the conversion of UO₂ to UC₂ began at the surface of the microsphere and progressed toward the central unreacted core. Kinetic models for solid state reactions in spheres were evaluated by using quantitative mass spectrometric data on the rate of evolution of carbon monoxide during conversion. This analysis revealed that the rate of conversion was controlled by reaction at the outer surface of the microsphere. Also, decreased partial pressures of carbon monoxide were found to accelerate the rate of reaction.

INTRODUCTION

The fissile fuel for High-Temperature Gas-Cooled Reactors is composed of uranium-bearing microspheres about 360 μm in diameter.¹ These microspheres or kernels are fabricated from uranium-loaded ion-exchange resin.^{2,3} Ion-exchange resins are utilized because of the ease of their fabrication in a remote system, the superior irradiation performance of such fuel, and the great versatility in the control of chemical and physical properties of the microspheres. A controlled heating to about 800°C in the absence of oxygen thermally decomposes the resin, removes all water, and leaves a very porous carbon matrix that contains finely dispersed UO₂. The kernels are then heated to 1500-1800°C in the absence of oxygen to carbothermally reduce the UO₂ according to the following overall reaction:



*Chemical Technology Division.

This reaction is not carried to completion because an overall composition of 65% UO_2 and 35% UC_2 plus a large excess of carbon is thought to give optimum irradiation performance.⁴ The relative proportions of UO_2 and UC_2 are determined by the conversion temperature, gas flow rate, fluidizing gas environment, charge size, and the reaction time.^{5,6} Since reaction mechanisms are not well understood, the extent of reaction is guided by past experience in that conditions that gave a certain percent conversion before are assumed to give the same percent conversion if repeated.

Earlier work assumed that the reaction of UO_2 with carbon occurred evenly throughout the microsphere since the UO_2 is finely dispersed in a very porous carbon matrix (Fig. 1). However, during a study to determine particle-to-particle variation in percent conversion, it was learned that the reaction does not proceed uniformly throughout the microsphere but begins at the outer surface and progresses toward the center (Fig. 1). This observation stimulated work to better understand the process and to determine the rate-controlling mechanisms.

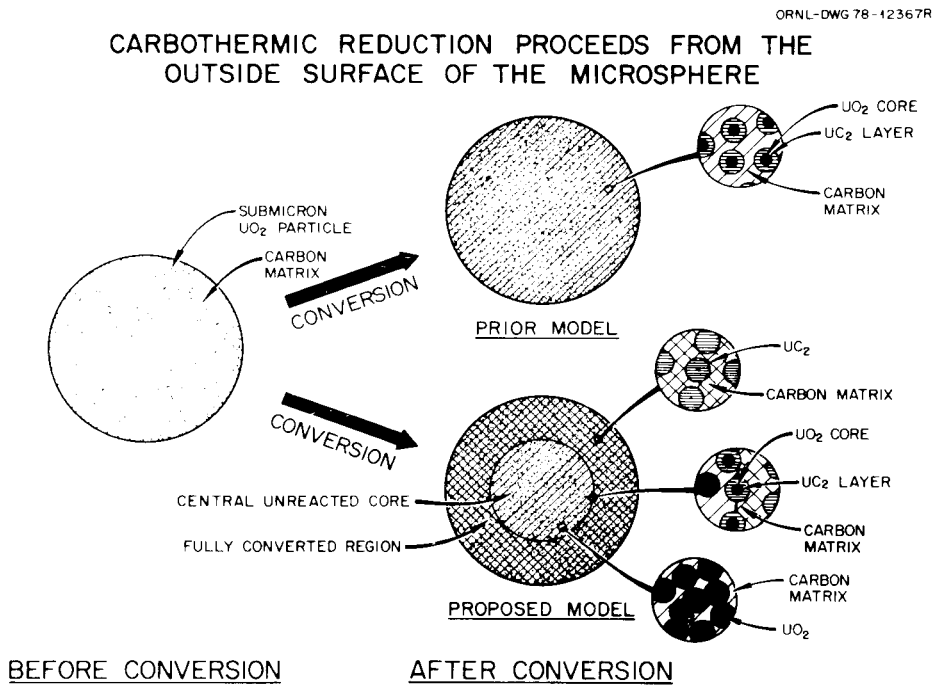


Fig. 1. Schematic showing the progression of the reaction of UO_2 to UC_2 by both the prior and the proposed models.

PROCEDURE

The furnace used for the conversion of UO_2 to UC_2 was a 13-cm-diam fluidized-bed furnace.⁷ The furnace is heated by a graphite electrical resistance heating element capable of reaching 1800°C . Normally, 500-g batches of particles are fluidized by argon passing through a porous plate gas distributor⁸ throughout the conversion process. During this experiment, both charge size and flow rate of argon were varied systematically for a total of nine runs (Fig. 2). Prior experience consisted of several hundred similar runs.

Four techniques were used to study the kinetics of the reaction between UO_2 and carbon. The first method was analysis of the gases liberated throughout the conversion process by use of an on-line time-of-flight mass spectrometer. Since the reaction, $\text{UO}_2 + 4\text{C} \rightarrow \text{UC}_2 + 2\text{CO}$, yields carbon monoxide as a product, the extent of the reaction can be easily followed by monitoring the carbon monoxide evolved. The products and reactants (UO_2 and UC_2) were studied by examining the x-ray diffraction patterns of the particles. Examination of the microstructures of the particles and an ion microprobe analysis also helped to define the rate-controlling mechanisms of the reaction.

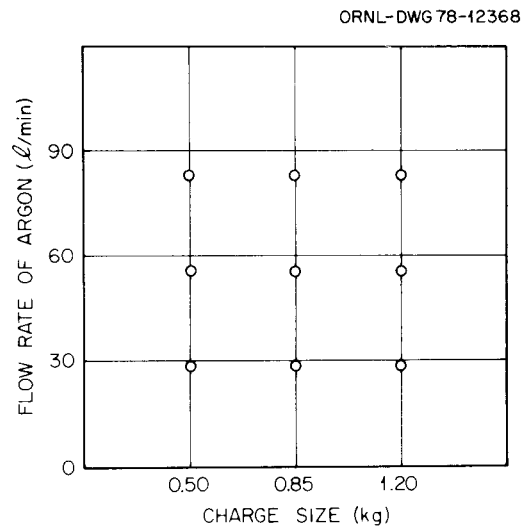


Fig. 2. Experimental plan used to determine the effect of charge size and argon flow rate on the reaction rate of UO_2 .

RESULTS AND DISCUSSION

Mass Spectrometry

The reaction mechanisms were examined in detail with the aid of a time-of-flight mass spectrometer. The mass spectrometer was used to monitor the effluents from seven of the nine conversion runs. These runs were all performed at about 1700°C with varying charge sizes and varying flow rates of argon as previously described. The samples were heated from room temperature to 1700°C in about 30 min and held at this temperature for 26 min. The major effluent shown by the mass spectrometer was carbon monoxide with a typical rate of evolution, as shown in Fig. 3. At about 1050°C, there was a small unexpected release of CO. Because the temperature was too low for the reaction of UO₂ and carbon, the CO

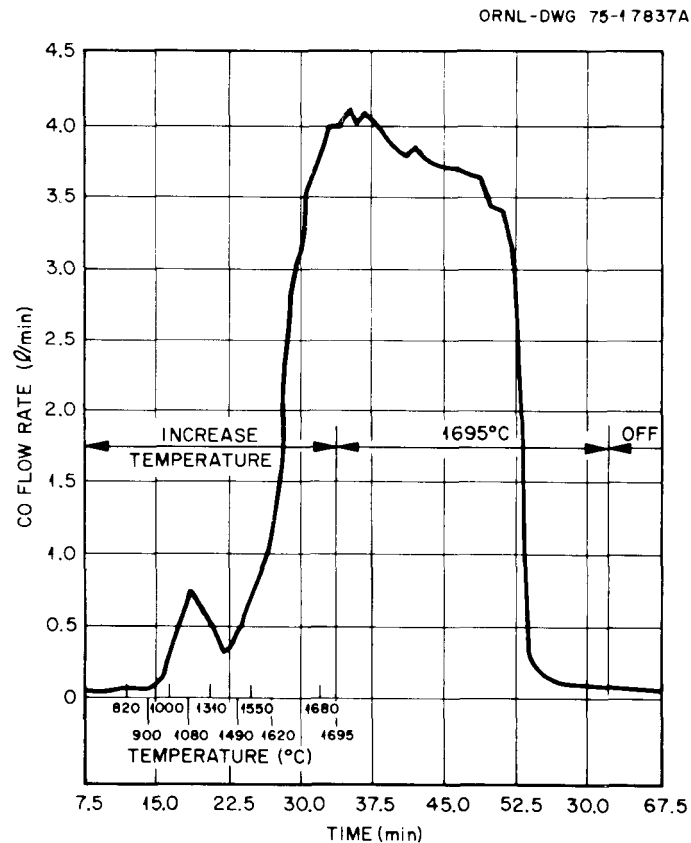


Fig. 3. Typical plot showing the evolution of carbon monoxide during a conversion run.

was suspected to be from the reduction of hyperstoichiometric UO_2 . As the temperature increased further, more CO was evolved until the reaction temperature was reached. During the 26 min at $1700^\circ C$, the rate of CO evolution gradually decreased. When nearly all the UO_2 had reacted, the evolution of CO decreased sharply. In some runs the temperature was reduced before the reaction went to completion. In these cases, the CO evolution decreased rapidly as the temperature was decreased. From the carbon monoxide releases-vs-time plot and the final percent conversion, as determined by subsequent oxygen analyses, the percent conversion at any given time could be calculated. The oxygen analyses were performed by reacting the oxygen with carbon and monitoring the products for carbon monoxide by infrared detection. The oxygen contents were verified by the difference from the carbon and uranium determinations. The accuracy of the oxygen analysis has been established as 0.5%.

Models for solid state reactions in spheres are given in the literature.⁹⁻¹⁴ These models apply when a product layer lies symmetrically over the reactant core. The reactants and products were spherically symmetrical in this study, as shown by metallography, x-ray diffraction, and the ion microprobe examinations to be discussed later. Results from a recent study¹⁵ of the uranium loss from coated resin particles confirmed that the reaction had proceeded from the outside of the kernel toward the inside. The models can be divided into three categories, depending on the controlling factors for the rate of reaction. The controlling factors are: (1) diffusion of a species through the product layer, (2) reaction at the inner product-reactant interface, and (3) reaction at the outer surface of the sphere.

The reaction is diffusion controlled if the limiting factor⁸⁻¹¹ is the removal of oxygen from the oxide core through the product layer by solid state diffusion. A model⁹ for diffusion control is

$$\frac{1}{3} - \left(\frac{r}{r_0}\right)^2 \left(1 - \frac{2r}{3r_0}\right) = K_D t / r_0^2, \quad (1)$$

where r is the average radius of the inner core of UO_2 at a given time and r_0 is the radius at time zero. The ratio r/r_0 was determined at

various times from geometric considerations since the percent conversion at any given time could be calculated from a plot of carbon monoxide flow rate vs time (Fig. 3) and the final percent conversion which was analytically determined. The proportionality constant is K_D and has units of cm^2/s . Since K_D and r_0 are constant, the left side of Eq. (1) must be equal to some constant multiplied by time if the reaction is diffusion controlled. The left side of Eq. (1) was plotted versus time for each conversion run. A typical plot for one of the conversion runs is shown in Fig. 4 by the closed circles. Time zero in this plot represents the time when the reaction temperature was reached. A small amount of conversion had already occurred; therefore, the curve does not go through the origin. The curve in Fig. 4 passes through point A at

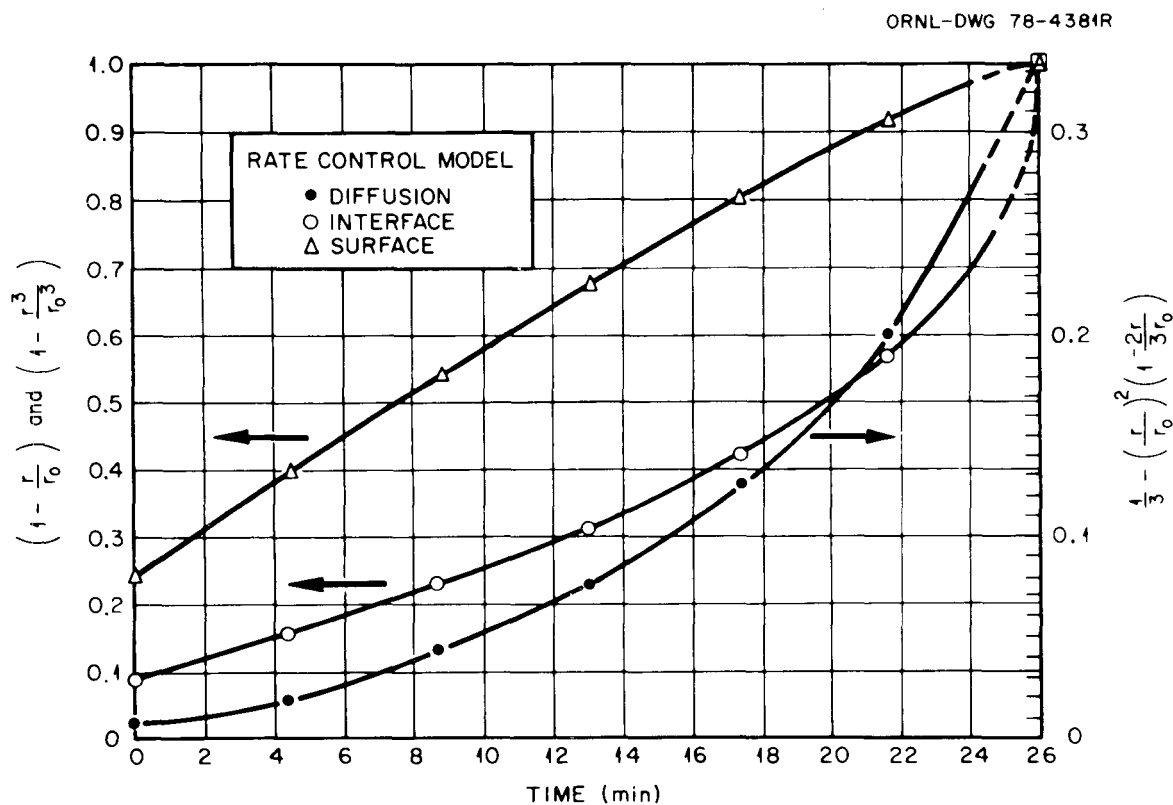


Fig. 4. Plot of three functions for rate-controlling mechanisms versus time. The plot for surface control is most linear, indicating that the reaction is largely surface controlled. Each curve passes through the point marked "A" because the material was 100% converted after 26 min.

26 min because this material was 100% converted at that time. Since such plots were not linear for any of the seven conversion runs, this is taken as evidence that the reaction is not diffusion controlled. Table I shows typical data as a function of time for percent conversion, r/r_0 , and reaction model calculations for the conversion depicted in Fig. 4. Data for the other conversion runs are available in the appendix.

Table I. Percent Conversion^α as a Function of Time; Calculations for Rate-Controlling Mechanisms

Time (min)	Conversion (%)	$\frac{r}{r_0}$	Interface Control $1 - \frac{r}{r_0}$	Surface Control $1 - \left(\frac{r}{r_0}\right)^3$	Diffusion Control $\frac{1}{3} - \left(\frac{r}{r_0}\right)^2 \left(1 - \frac{2r}{3r_0}\right)$
0.0	24	0.912	0.088	0.2414	0.0073
4.3	40	0.843	0.157	0.4009	0.0221
8.7	54	0.772	0.228	0.5399	0.0441
13.0	67	0.691	0.309	0.6701	0.0758
17.3	80	0.584	0.416	0.8008	0.1251
21.7	92	0.430	0.570	0.9205	0.2014
26.5	100	0.000	1.000	1.0000	0.3333

^αRun 1 (0.50 kg U, 28 liters/min Ar).

The reaction may also be controlled by reaction at the interface of the UC_2 and UO_2 .^{9,13} The model⁹ that describes interface control is

$$1 - \frac{r}{r_0} = K_I t / r_0, \quad (2)$$

where K_I is a constant expressed in centimeters/second and the other terms are as previously defined. Since K_I and r_0 are constant, $1 - r/r_0$ can be equated to a constant multiplied by time if the reaction is interface controlled. A straight line will be obtained if $1 - r/r_0$ is plotted against time, provided the reaction is interface controlled. This function is plotted in Fig. 4 as open circles. A straight line was

not obtained. Similar plots for the other conversion runs were also nonlinear; therefore, the reaction must not be interface controlled.

The final reaction mechanism is surface control.^{10,14} This model is described by the equation

$$1 - \left(\frac{r}{r_0}\right)^3 = 3k_s t/r_0 . \quad (3)$$

The constant k_s is expressed in centimeters/second. Again, since $3k_s$ and r_0 are constant, $1 - (r/r_0)^3$ must be proportional to time if the reaction is actually surface controlled. This function is plotted in Fig. 4 with triangles, and the resulting line is nearly straight. Plots for the other conversion runs were also straight up to nearly 100% conversion. The reaction, therefore, appears to be mainly surface controlled. A typical batch of converted particles has a mean diameter of 360 μm , but the size varies from 330 to 390 μm . Assuming the surface-controlled model is obeyed, then this variation in size would cause the percent conversion from particle to particle to vary from 60 to 72% if the average 360- μm particle were converted to 65%.

Several batches of microspheres were examined that were converted using a constant batch size but varying argon flow (different partial pressures of carbon monoxide). The percent conversion is plotted against time for three runs (Fig. 5). The flow rates of argon were 28, 57, and 85 liter/min. As determined from Fig. 5, the lowest argon flow rate (highest partial pressure of CO) yielded a conversion rate of 3.23%/min. When a 57-liter/min flow was used, the rate increased to 5.64%/min, and the highest flow rate of argon (lowest partial pressure of CO) yielded the fastest rate of 6.25%/min. Therefore, the reduced partial pressures of carbon monoxide increased the rate of reaction. These results appear to indicate that carbon monoxide diffuses through a thin layer at the surface of the microsphere. This gives apparent surface control; however, the surface mechanism is diffusion because the diffusion rate is proportional to the gradient in CO partial pressure across the thin surface layer. However, the reaction is not entirely surface controlled since

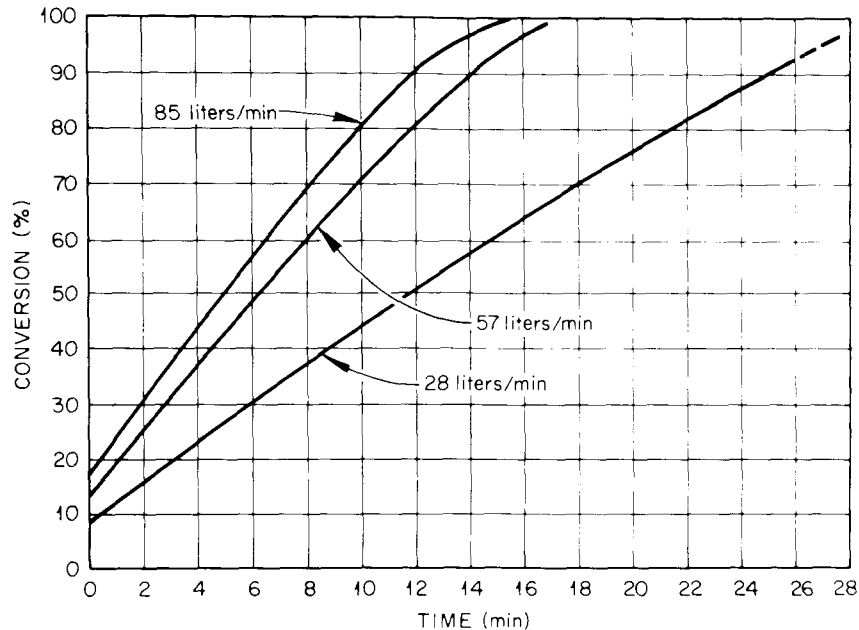


Fig. 5. Correlation of percent conversion with time. The correlation shows that an increase in argon flow rate increases the reaction rate. A charge of 500 g was used for all runs.

the reaction rate decreases slightly as the percent conversion increases (Fig. 5). If it were, the rate of reaction would remain constant throughout the conversion process.

X-Ray Diffraction

Results obtained from x-ray diffraction measurements indicated that the reaction of UO_2 to UC_2 did not proceed uniformly throughout the microsphere. An individual microsphere from a converted batch was sealed in a glass capillary, and a Debye-Scherrer x-ray diffraction pattern was made from crystal monochromatized CuK_α radiation. These results primarily indicated the composition of the outer few microns of the microsphere. The processed films measured by a precision densitometer showed that the microsphere contained no UO_2 , so complete conversion had occurred. This disagreed with a precise analytical determination of the overall oxygen content of samples that consisted of several thousand

particles. The bulk oxygen determination found sufficient oxygen to correspond to a mixture of 55% UC_2 and 45% UO_2 . When the particle was crushed and again analyzed by x-ray diffraction, the overall percent conversion found was much closer to that determined analytically. This procedure was repeated on numerous conversion runs with similar results. These results indicate that the outer portion of the microspheres contains less UO_2 and more UC_2 than the inner portion does. It was concluded that conversion to UC_2 had occurred first at the outer surface of the microsphere and then gradually progressed toward the central core, which contained unreacted UO_2 (Fig. 1).

Metallography

Microspheres were metallographically examined to find a boundary between UO_2 and UC_2 areas. Samples were prepared by mounting microspheres in epoxy and polishing them down to their midplane. The polished sample was then etched with equal parts of water, nitric acid, and acetic acid to reveal the various layers. Distinct layers could easily be found in converted samples (Fig. 6). It is assumed that the outer layer in the

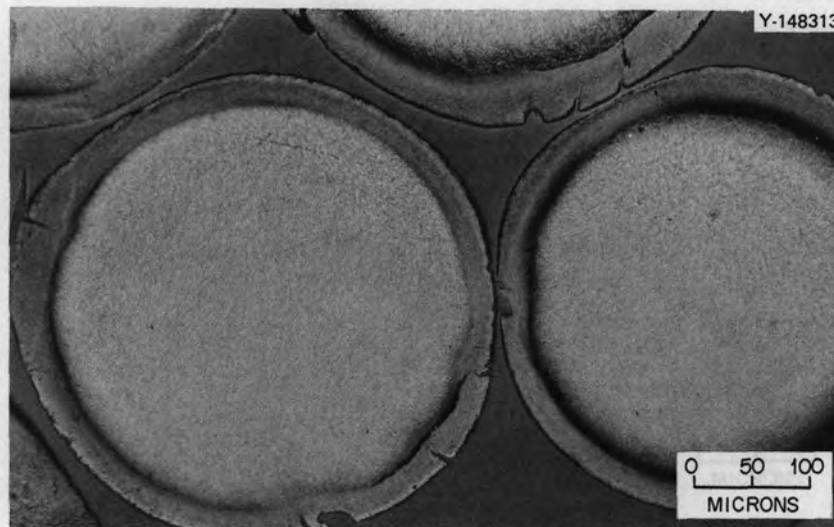


Fig. 6. Distinct layers are present in converted microspheres. Because the material is pyrophoric, samples have oxidized slightly, especially between the two layers.

photograph is $UC_2 + C$, and the inner layer is $UO_2 + C$. When fully converted samples (100% UC_2) were examined, the microstructure still revealed a layered structure; however, more than two layers were present. The compositions of the different layers were not known. The distinct layers that were observed confirm that the reaction did not occur uniformly throughout the microsphere. It should be pointed out that the starting resin appeared uniform and was not layered. The layers apparent in Fig. 6 were not visible even in converted material until etched to differentiate between carbide and oxide.

Ion Microprobe

An ion microprobe mass analyzer* was used to search for gradients of oxygen, UO_2 , or UC_2 across a metallographically polished section. Both positive and negative secondary ion mass spectra from cross sections through the midplane of the particles were investigated. An apparent oxygen gradient across the kernel cross section was detected. More oxygen appeared at the center of the kernels than near the periphery for a 71%-converted specimen. This confirms the results of x-ray diffraction and metallography that the reaction proceeds from the outside of the particle. Many particles of different conversion levels were examined, but it was impossible to identify distinct layers or to quantitatively determine the composition of the various layers detected by metallography.

CONCLUSIONS

From the analyses using metallography, ion microprobe, and x-ray diffraction, it was concluded that the reaction between finely dispersed UO_2 in a porous carbon matrix proceeded from the outside surface toward the center of the sphere. This formed a layer of $UC_2 + C$ that surrounded the inner core of $UO_2 + C$. Mass spectrometer results helped to show that the reaction was largely surface controlled. This was quite surprising because other studies that used dense UO_2 microspheres reacting with

*Manufactured by Applied Research Laboratories, Sunland, California.

carbon were diffusion controlled.^{9,13} Since the microspheres were composed of a very porous carbon matrix, carbon monoxide understandably would diffuse easily through the layer of UC_2 that had formed, so the reaction would not be diffusion controlled. A surface-controlled reaction implies that something occurs at the surface of the sphere which controls the reaction. Perhaps a thin layer forms at the surface during processing of the weak-acid resin and inhibits the flow of carbon monoxide across the boundary.

The reaction of finely dispersed UO_2 in a porous carbon microsphere formed from a weak-acid resin is mainly surface controlled. This surface-controlled reaction can be affected by the reaction temperature and the flow rate of argon through the fluidized bed.

ACKNOWLEDGMENTS

The authors wish to express their appreciation to D. R. Johnson whose interest and helpful suggestions helped carry this work to completion. We also are grateful to D. A. Lee for his careful work in monitoring the conversion runs using the mass spectrometer. We also would like to thank D. A. Castanzo for providing the chemical analysis.

REFERENCES

1. J. D. Sease and A. L. Lotts, "Development of Processes and Equipment for the Refabrication of HTGR Fuels," DOE Rept. ORNL/TM-5334, June 1976.
2. P. A. Haas, J. P. Drago, D. L. Million, and R. D. Spence, "Development, Design, and Preliminary Operation of a Resin-Feed Processing Facility for Resin-Based HTGR Fuels," DOE Rept. ORNL/TM-6061, Jan. 1978.
3. P. A. Haas, "Resin-Based Preparation of HTGR Fuels; Operation of an Engineering-Scale Uranium Loading System," DOE Rept. ORNL-5300, Oct. 1977.
4. F. J. Homan, T. B. Lindemer, E. L. Long, Jr., T. N. Tiegs, and R. L. Beatty, "Stoichiometric Effects on Performance of High-Temperature Gas-Cooled Reactor Fuels from the U-C-O System," *Nucl. Technol.*, 35 [2] 428 (1977).

5. D. R. Johnson, W. J. Lackey, and J. D. Sease, "The Effects of Processing Variables on HTGR Fuel Kernels Fabricated from Uranium Loaded Cation-Exchange Resin," *Am. Ceram. Soc. Bull.*, 56 [6] 567-71 (1977).
6. G. W. Weber, R. L. Beatty, and V. J. Tennery, "Processing and Composition Control of Weak-Acid-Resin-Derived Fuel Microspheres," *Nucl. Technol.*, 35 [2] 217 (1977).
7. R. B. Pratt, J. D. Sease, W. H. Pechin, and A. L. Lotts, "Pyrolytic Carbon Coating in an Engineering-Scale System," *Nucl. Appl.*, 6 [3] 241-55 (1969).
8. W. J. Lackey, D. P. Stinton, and J. D. Sease, "Improved Gas Distributor for Coating High-Temperature Gas-Cooled Reactor Fuel Particles," *Nucl. Technol.*, 35 [2] 227-37 (1977).
9. T. B. Lindemer, M. D. Allen, and J. M. Leitnaker, "Kinetics of the Graphite-Uranium Dioxide Reaction from 1400°C to 1756°C," *J. Am. Ceram. Soc.*, 52 [5] 233-37 (1969).
10. G. Danger and S. Besson, "Kinetic Study of the Carboreduction of Uranium Dioxide," *J. Nucl. Mater.*, 54 190-98 (1974).
11. R. E. Carter, "Kinetic Model for Solid State Reactions," *J. Chem. Phys.*, 34 [6] 2010-15 (1961).
12. R. E. Carter, "Addendum: Kinetic Model for Solid-State Reactions," *J. Chem. Phys.*, 35 [3] 1137-38 (1961).
13. T. B. Lindemer, "Rate Controlling Factors in the Carbothermic Synthesis of Advanced Fuels," *Nucl. Appl. Technol.*, 9 711-15 (1970).
14. T. B. Lindemer, J. M. Leitnaker, and M. D. Allen, "Kinetics of the Reaction of UC_2 and Nitrogen from 1500° to 1700°C," *J. Am. Ceram. Soc.*, 53 [8] 451-56 (1970).
15. R. L. Pearson and T. B. Lindemer, "Uranium Loss from Biso-Coated Weak-Acid-Resin HTGR Fuel," DOE Rept. ORNL/TM-5552 (Feb. 1977).

APPENDIX

Table A.1. Data Showing Reaction Kinetics
of Six Conversion Runs at 1700°C

Time (min)	Conversion (%)	$\frac{r}{r_0}$	Interface Control $1 - \frac{r}{r_0}$	Surface Control $1 - \left(\frac{r}{r_0}\right)^3$	Diffusion Control $\frac{1}{3} - \left(\frac{r}{r_0}\right)^2 \left(1 - \frac{2r}{3r_0}\right)$
<u>Run 2: 500 g U, 57 liters/min Ar</u>					
0.0	12.54	0.956	0.044	0.1263	0.0019
2.1	26.48	0.903	0.097	0.2637	0.0088
4.2	39.36	0.846	0.154	0.3945	0.0213
6.3	51.43	0.780	0.214	0.5144	0.0413
8.4	62.68	0.720	0.280	0.6268	0.0638
10.5	73.21	0.645	0.355	0.7317	0.0962
12.6	83.20	0.552	0.448	0.8318	0.1408
14.7	93.56	0.401	0.599	0.9355	0.2155
16.8	98.82	0.228	0.772	0.9881	0.2893
<u>Run 3: 500 g U, 85 liters/min Ar</u>					
0.0	16.9	0.940	0.060	0.1694	0.0035
1.98	30.3	0.887	0.113	0.3021	0.0118
3.95	42.9	0.830	0.170	0.4282	0.0256
5.93	55.8	0.762	0.238	0.5575	0.0477
7.90	68.5	0.680	0.320	0.6856	0.0806
9.88	80.1	0.584	0.416	0.8008	0.1251
11.85	90.6	0.455	0.545	0.9058	0.1891
13.83	97.1	0.306	0.694	0.9713	0.2588
15.80	100.0	0.000	1.000	1.0000	0.3333
<u>Run 4: 850 g U, 28 liters/min Ar</u>					
0.0	9.9	0.966	0.034	0.0986	0.0011
2.33	16.5	0.942	0.058	0.1641	0.0032
4.67	23.1	0.916	0.084	0.2314	0.0067
7.00	29.6	0.890	0.110	0.2950	0.0112
9.33	36.0	0.862	0.138	0.3595	0.0173
11.67	42.2	0.833	0.167	0.4220	0.0248
14.00	48.3	0.803	0.197	0.4822	0.0337
16.33	54.2	0.771	0.229	0.5417	0.0444
18.67	59.9	0.738	0.262	0.5981	0.0567
21.00	65.4	0.702	0.298	0.6541	0.0712
23.33	70.6	0.669	0.331	0.7006	0.0854
25.67	75.5	0.626	0.374	0.7547	0.1050
28.00	80.0	0.585	0.415	0.7998	0.1246
30.33	84.1	0.542	0.458	0.8408	0.1457

Table A.1 (continued)

Time (min)	Conversion (%)	$\frac{r}{r_0}$	Interface Control $1 - \frac{r}{r_0}$	Surface Control $1 - \left(\frac{r}{r_0}\right)^3$	Diffusion Control $\frac{1}{3} - \left(\frac{r}{r_0}\right)^2 \left(1 - \frac{2r}{3r_0}\right)$
<u>Run 5: 850 g U, 57 liters/min Ar</u>					
0.0	7.16	0.976	0.024	0.0703	0.0006
2.17	9.60	0.967	0.033	0.0958	0.0011
4.33	12.11	0.958	0.042	0.1208	0.0017
6.50	14.52	0.949	0.051	0.1453	0.0025
8.67	16.86	0.940	0.060	0.1694	0.0035
10.83	19.19	0.931	0.069	0.1930	0.0045
13.00	21.52	0.922	0.078	0.2162	0.0058
15.17	23.85	0.913	0.087	0.2390	0.0071
17.33	26.15	0.904	0.096	0.2612	0.0086
19.50	28.41	0.895	0.105	0.2831	0.0103
21.67	30.65	0.885	0.115	0.3068	0.0122
23.83	32.64	0.877	0.123	0.3255	0.0139
<u>Run 6: 1200 g U, 28 liters/min Ar</u>					
0.0	13.73	0.952	0.048	0.1372	0.0022
2.13	18.29	0.935	0.065	0.1826	0.0040
4.27	22.79	0.917	0.083	0.2289	0.0065
6.40	27.13	0.899	0.101	0.2734	0.0095
8.53	31.27	0.882	0.118	0.3139	0.0128
10.67	35.31	0.865	0.135	0.3528	0.0166
12.80	39.27	0.847	0.153	0.3924	0.0210
14.93	43.12	0.829	0.171	0.4303	0.0259
17.07	46.94	0.808	0.192	0.4725	0.0322
19.20	50.75	0.789	0.211	0.5088	0.0383
21.34	54.53	0.768	0.232	0.5470	0.0455
23.47	58.29	0.747	0.253	0.5832	0.0532
25.60	61.99	0.724	0.276	0.6205	0.0622
27.74	65.35	0.702	0.298	0.6541	0.0712
<u>Run 7: 1200 g U, 57 liters/min Ar</u>					
0.0	7.10	0.976	0.024	0.0081	0.0006
2.05	14.10	0.951	0.049	0.1399	0.0023
4.10	22.65	0.918	0.082	0.2264	0.0064
6.15	30.71	0.885	0.115	0.3068	0.0122
8.20	38.53	0.850	0.150	0.3859	0.0203
10.25	46.26	0.813	0.187	0.4626	0.0306
12.30	53.64	0.774	0.226	0.5363	0.0434
14.35	60.66	0.733	0.267	0.6062	0.0586
16.40	67.68	0.686	0.314	0.6772	0.0780
18.45	74.51	0.634	0.366	0.7452	0.1013

Table A.1 (continued)

Time (min)	Conversion (%)	$\frac{r}{r_0}$	Interface Control $1 - \frac{r}{r_0}$	Surface Control $1 - \left(\frac{r}{r_0}\right)^3$	Diffusion Control $\frac{1}{3} - \left(\frac{r}{r_0}\right)^2 \left(1 - \frac{2r}{3r_0}\right)$
<u>Run 7: 1200 g U, 57 liters/min Ar</u>					
20.50	81.00	0.575	0.425	0.8099	0.1295
22.55	87.08	0.506	0.494	0.8704	0.1637
24.60	92.71	0.418	0.582	0.9270	0.2073
26.65	97.27	0.301	0.699	0.9727	0.2609

ORNL/TM-6589
Dist. Category UC-77

INTERNAL DISTRIBUTION

1-2.	Central Research Library	30.	K. H. Lin
3.	Document Reference Section	31-35.	T. B. Lindemer
4-5.	Laboratory Records Department	36.	E. L. Long, Jr.
6.	Laboratory Records Department, ORNL-RC	37.	J. E. Mack
7.	ORNL Patent Section	38.	A. P. Malinauskas
8.	P. Angelini	39.	A. D. Mitchell
9.	R. L. Beatty	40.	K. J. Notz
10.	E. S. Bomar	41.	A. E. Pasto
11.	J. L. Botts	42.	R. L. Pearson
12.	A. J. Caputo	43.	H. E. Reesor
13.	O. B. Cavin	44.	J. E. Selle
14.	W. P. Eatherly	45.	R. D. Spence
15.	J. I. Federer	46-50.	D. P. Stinton
16.	P. A. Haas	51.	R. R. Suchomel
17-18.	M. R. Hill	52-56.	S. M. Tiegs
19.	F. J. Homan	57.	T. N. Tiegs
20.	D. R. Johnson	58.	R. W. Balluffi (consultant)
21.	R. R. Judkins	59.	P. M. Brister (consultant)
22-23.	P. R. Kasten	60.	W. R. Hibbard, Jr. (consultant)
24-28.	W. J. Lackey	61.	M. J. Mayfield (consultant)
29.	D. A. Lee	62.	N. E. Promisee (consultant)
		63.	J. T. Stringer (consultant)

EXTERNAL DISTRIBUTION

64-65. DOE DIVISION OF NUCLEAR POWER DEVELOPMENT, Washington, DC 20545
Director

66. SAN-DEVELOPMENT, SAN DIEGO AREA OFFICE, P.O. Box 81325, San Diego, CA 92138
Senior Program Coordinator

67. DOE SAN FRANCISCO OPERATIONS OFFICE, 1333 Broadway, Wells Fargo Building, Oakland, CA 94612
Manager

68. DOE OAK RIDGE OPERATIONS OFFICE, P.O. Box E, Oak Ridge, TN 37830
Assistant Manager, Energy Research and Development

69-245. DOE TECHNICAL INFORMATION CENTER, P.O. Box 62, Oak Ridge, TN 37830
For distribution as shown in TID-4500 Distribution Category, UC-77 (Gas-Cooled Reactor Technology)